© 2014. Published by The Company of Biologists Ltd | Development (2014) 141, 3793-3798 doi:10.1242/dev.109637

RESEARCH REPORT

TECHNIQUES AND RESOURCES

Systematic profiling of spatiotemporal tissue and cellular stiffness in the developing brain

Misato Iwashita[1], Noriyuki Kataoka[2], Kazunori Toida[1] and Yoichi Kosodo[1,*]

ABSTRACT

Accumulating evidence implicates the significance of the physical properties of the niche in influencing the behavior, growth and differentiation of stem cells. Among the physical properties, extracellular stiffness has been shown to have direct effects on fate determination in several cell types *in vitro*. However, little evidence exists concerning whether shifts in stiffness occur *in vivo* during tissue development. To address this question, we present a systematic strategy to evaluate the shift in stiffness in a developing tissue using the mouse embryonic cerebral cortex as an experimental model. We combined atomic force microscopy measurements of tissue and cellular stiffness with immunostaining of specific markers of neural differentiation to correlate the value of stiffness with the characteristic features of tissues and cells in the developing brain. We found that the stiffness of the ventricular and subventricular zones increases gradually during development. Furthermore, a peak in tissue stiffness appeared in the intermediate zone at E16.5. The stiffness of the cortical plate showed an initial increase but decreased at E18.5, although the cellular stiffness of neurons monotonically increased in association with the maturation of the microtubule cytoskeleton. These results indicate that tissue stiffness cannot be solely determined by the stiffness of the cells that constitute the tissue. Taken together, our method profiles the stiffness of living tissue and cells with defined characteristics and can therefore be utilized to further understand the role of stiffness as a physical factor that determines cell fate during the formation of the cerebral cortex and other tissues.

KEY WORDS: Atomic force microscopy, Elasticity, Mechanical property, Embryonic tissue, Brain development, Cerebral cortex, Mechanotransduction, Neural stem cells, Mouse

INTRODUCTION

During development, somatic stem cells define specific niches within different tissues to control their cellular environment. Accumulating evidence indicates the significance of the physical properties of the niche for influencing cellular behavior, growth and differentiation. The process of how physical stimuli are sensed and subsequently translated into biochemical signals by cells in a specific niche is referred to as mechanotransduction (DuFort et al., 2011; Hoffman et al., 2011). Among mechanical stimuli, the stiffness of the surrounding niche has been implicated to have ubiquitous roles in the determination of cell fates of various somatic stem cells, including mesenchymal (Engler et al., 2006) and muscle stem cells (Gilbert et al., 2010). These results, which have been acquired from *in vitro* culture studies, suggest that stem cells can sense the shift in stiffness of the surrounding tissue and then determine their final fate during development. However, crucial information is lacking to reconcile this hypothesis with the developmental program, owing to the lack of knowledge about the spatiotemporal shift in stiffness in the developing tissue. Whether there are shifts in stiffness in a given niche and, importantly, whether the shifts are correlated with cell fate determination *in vivo* need to be clarified in order to understand the stiffness-based mechanotransduction in tissue formation.

To address this point, we present a systematic strategy to evaluate the shift in stiffness in developing tissue using the mouse embryonic cerebral cortex as an experimental model. The developing cortex has the following advantages to render it a suitable model for studying *in vivo* mechanotransduction: (1) the lineages from undifferentiated neural stem and progenitor cells to terminally differentiated neurons are well characterized (Götz and Huttner, 2005; Lui et al., 2011), and (2) during brain formation, several layered structures appear in the cortex, and the physical characteristics within each layer are likely to be different according to the proper cytoarchitecture (Fujita, 2003). Thus, investigating the correlation between the neural cell lineage and the temporal shift in the stiffness of each layer in the cortex might reveal the role of stiffness in cell fate determination.

The brain is one of the softest tissues in the human body (Moore et al., 2010; Spedden et al., 2012). Its stiffness in the postnatal stage has been examined previously in the rodent cerebral cortex (Elkin et al., 2010), the hippocampus (Elkin et al., 2007) and the cerebellum (Christ et al., 2010), although it has never been measured at developing stages (Franze, 2013). Interestingly, previous studies have demonstrated that culturing mesenchymal stem cells (Engler et al., 2006) and human pluripotent stem cells (Keung et al., 2012) on material that mimics the softness of the brain results in the induction of neural fate. Moreover, lineage switching from neural to glial cells can be influenced by the shift of substrate stiffness (Saha et al., 2008; Leipzig and Shoichet, 2009). To address whether these *in vitro* studies reflect bona fide fate determination in the developing cortex, the spatiotemporal profiling of stiffness *in vivo* needs to be demonstrated. Our systematic examinations presented here successfully represent a substantial technical achievement and provide information concerning the shift in stiffness in the developing cortex through comparison of the stiffness of the tissue layers with that of the single cells at different neural differentiation states. These experimental strategies can be used to further understand the role of stiffness as a physical factor for somatic stem cell fate determination during the formation of the cerebral cortex and other tissues.

RESULTS AND DISCUSSION

Strategies for the systematic profiling of the stiffness of tissues and cells freshly harvested from the developing brain

To measure the mechanical properties of the developing brain, we designed the following approaches: Brain slices obtained from

[1]Department of Anatomy, Kawasaki Medical School, Kurashiki 701-0192, Japan. [2]Department of Medical Engineering, Kawasaki University of Medical Welfare, Kurashiki 701-0193, Japan.

*Author for correspondence (kosodo@med.kawasaki-m.ac.jp)

Received 27 February 2014; Accepted 1 August 2014

Development (2014) 141, 3793-3798 doi:10.1242/dev.109637

embryos at several different stages of development were quickly prepared, and the Young's modulus, a physical value that represents stiffness, was obtained using atomic force microscopy (AFM). We noted that the conventional slice preparation method, which has been used for previous AFM measurements of postnatal brain tissue (Elkin et al., 2007; Christ et al., 2010), was not suitable to maintain an intact tissue structure because of the fragility of embryonic brain (supplementary material Fig. S2A). To overcome this problem, we embedded living brain tissue into agar, followed by the preparation of 250-μm-thick sections with agar as a frame, which maintains the tissue structure during AFM measurements (Fig. 1A). The concentration of agar did not affect the tissue stiffness (supplementary material Fig. S2B).

The developing brain showed massive expansion (Fig. 1B), and the dorsal cortex formed a multi-layered structure (Fig. 1C). Using the improved AFM method, we designed experiments to examine the stiffness of the layers in the coronal cortical slices at four different stages (E12.5, E14.5, E16.5 and E18.5), the major neurogenic periods in the dorsal cortex (Molyneaux et al., 2007). For AFM measurements, we applied an AFM probe with a bead to points that

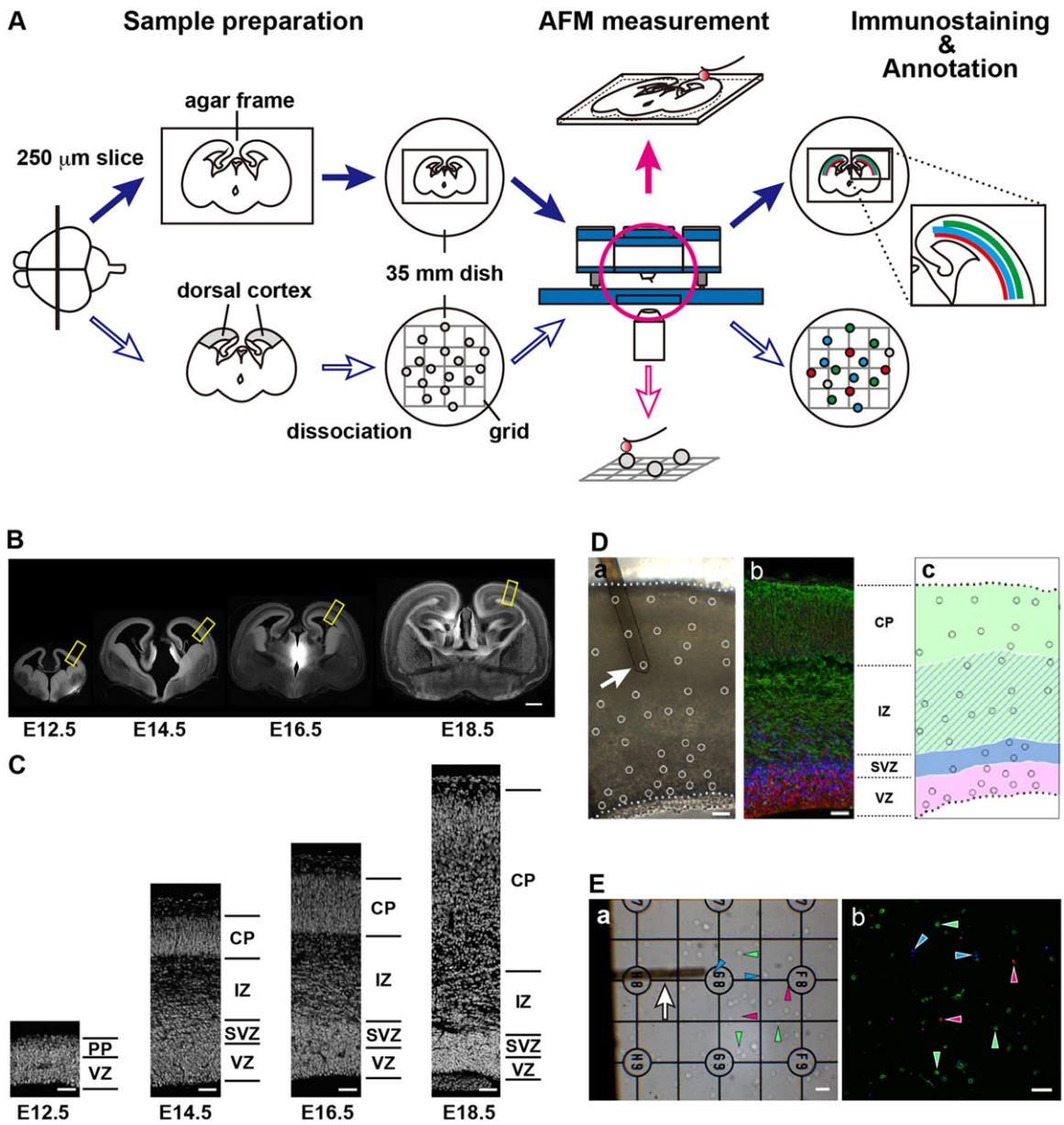

Fig. 1. Overview of the AFM experiments. (A) Schematic diagram of the experiments. (B) Coronal sections prepared from brains at different embryonic stages (E12.5, E14.5, E16.5 and E18.5). Yellow rectangles indicate the measured region in the dorsal cortices shown in C. White, nuclei. (C) Embryonic dorsal cortex exhibits stratification during brain development. In the early stages of corticogenesis (E12.5), the VZ and preplate (PP) were observed. The SVZ and IZ appeared at E14.5 and extended toward E16.5. At E18.5, the VZ, SVZ and IZ became narrower, whereas the CP expanded. White, nuclei. The ventricular surface is towards the bottom of the image. (D) Procedure to measure the tissue stiffness of the cortical slices. Measured points in the dorsal cortex were plotted on the bright-field images (a). Immunostaining (b) was then performed to categorize each plotted point (c). (a) Arrow, cantilever. (b) Red, Pax6; blue, Tbr2; green, Tuj1. (E) Procedure to measure the stiffness of a single cell. (a) Dissociated cells were cultured on a grid-lined dish for identification. Arrow, cantilever. (b) Subsequent to the measurement of stiffness, the cells were classified by markers of neural differentiation. Arrowheads in a and b indicate the same cells (red, Pax6; blue, Tbr2; green, Tuj1). Scale bars: 500 μm in B; 50 μm in C-E.

Development (2014) 141, 3793-3798 doi:10.1242/dev.109637

were dispersed throughout the cortical region (Fig. 1D). The Young's modulus corresponding to each point was then calculated from the obtained force-distance curves. We found that the Young's moduli at all of the chosen stages of development exhibited an indentation depth-dependent stiffening with the exception of a decrease at smaller (~0.5 µm) depths (supplementary material Fig. S3), as observed previously in a study of the stiffness of the postnatal hippocampus (Elkin et al., 2007). As a result, we have successfully optimized a protocol that uses AFM to measure the stiffness of particularly soft tissue.

Cortical tissue layers show significant shifts in stiffness during brain development

In order to profile the mechanical properties of the embryonic brain in greater detail, we next sought to ascertain the value of stiffness at each state of neural differentiation. For this purpose, we performed immunostaining of cortical slices after AFM measurements, and the position at which the stiffness was measured was overlaid with the immunohistological information (Fig. 1D), a method that has not been reported in previous studies of developing or postnatal brain tissue (Franze, 2011; Spedden and Staii, 2013). We took advantage of the structural support provided by the agar frame surrounding the sliced brain in order to manipulate the soft tissues in fixation and immunohistochemistry analyses (Fig. 1A). We performed triple immunostaining with antibodies against Pax6, Tbr2 (Eomes – Mouse Genome Informatics) and Tuj1 (Tubb3 – Mouse Genome Informatics), markers that are consecutively expressed during neural differentiation in the dorsal cortex (Fig. 1D) (Hevner et al., 2006). Pax6 is expressed in the apical progenitors in the ventricular zone (VZ). Tbr2 is expressed in the intermediate progenitors, a progenitor subtype that is generated from an apical progenitor, in the subventricular zone (SVZ) and partially in the intermediate zone (IZ). Both progenitors differentiate into neurons that comprise the IZ and the cortical plate (CP).

We then undertook a systematic profiling of the stiffness of the layers that appeared during the formation of the cortex (Fig. 2; Table 1) at an indentation depth of 3 µm (supplementary material Fig. S3). Remarkably, we found that all layers of the developing cortex showed significant changes in stiffness throughout the different embryonic stages. In the VZ and SVZ, the Young's moduli increased gradually, exhibiting the highest value at E18.5 [149.3±15.0 and 169.3±18.7 Pa (mean±s.e.m.) in the VZ and the SVZ, respectively]. A prominent peak appeared in the IZ at E16.5, which showed the greatest stiffness (216.7±23.4 Pa) among the layers examined. In the CP, the Young's modulus was lower at E18.5 (57.4±7.7 Pa) than in the middle stages of neurogenesis (108.4±14.9 Pa in E16.5). Thus, we have successfully created a novel procedure to determine the tissue stiffness discernible by the characteristic features of each tissue region, and have documented for the first time that layers in the developing cortex show temporal shifts in stiffness.

Neurons, but not neural progenitors, show a significant shift in stiffness throughout the developmental stages

We further explored the possibility of whether the identified shift in the stiffness of the developing brain could be attributed to changes in the stiffness of the neural cells that comprise each cortical layer. For a systematic measurement of single cell stiffness, we improved the method that has been used previously to study the structural details of subcellular compartments, such as growth cones, by combining AFM with immunocytochemistry (Kondra et al., 2009). We dissociated cortical cells from each of the different stages of development and plated the cells on a grid-lined glass-bottomed dish in order to measure stiffness using AFM (Fig. 1A,E). We next tested different dish-coating conditions, and strikingly, found that differences in the extracellular matrix (ECM) used for coating the dish influenced the stiffness of cortical cells (supplementary material Fig. S4A). Coating with poly-L-ornithine and fibronectin allowed a fine linearity along the indentation depth (supplementary material Fig. S4B). We chose 5% of the cell height (8.7±0.2 µm, n=48) as the indentation depth for further analyses because of the fine linearity in the range of 2.5 to 10% of the cell height at all of the developmental stages that we tested (supplementary material Fig. S5).

To correlate the cellular stiffness with the differentiation state in the neural lineage, immunocytochemistry analyses of the cells that had been measured were subsequently performed using antibodies against Pax6, Tbr2 and Tuj1 and the grid-lined dish to match the results of each analysis for a specific cell (Fig. 1E; Fig. 3A). Analysis of the cell populations throughout the developing stages yielded the following findings (Fig. 3B): (1) The proportions of the dissociated cells apparently corresponded to the thickness of the layers that were positive for the same markers at each stage of development (Fig. 2A), which suggests that the dissociation and culture of neural cells did not greatly influence their differentiation state. (2) The majority (92-97%) of cells are in the neural lineage (Fig. 3B, positive for Pax6, Tbr2 or Tuj1 staining), indicating that neural cells [including Pax6-positive radial glial cells (Götz et al., 1998)] provide a major contribution to tissue stiffness. (3) Remarkably, we found that Pax6-positive apical progenitors and Tbr2-positive intermediate progenitors exhibited small shifts in stiffness during development. By contrast, the stiffness of the neurons increased monotonically throughout the progression of development; 154.7±11.8 (E12.5) to 230.5±20.0 Pa (E18.5) (Fig. 3C; Table 1). A previous report has indicated that the stabilization of microtubules contributes to the increase in the stiffness of a cortical neuron (Spedden et al., 2012), raising the possibility that the stiffness of neural cells is determined by the status of the microtubule cytoskeleton. This notion is supported by the increasing amount of tubulin β III (Tuj1) in the soma during neural maturation (Fig. 3A). Furthermore, using nocodazole to interfere with microtubule polymerization decreased the stiffness of embryonic cortical cells both at the earlier and later stages of development (Fig. 3D). These results indicate that the maturation of the microtubule cytoskeleton is responsible for the increasing stiffness in neurons during embryonic development.

Here, we have established a methodology for the systematic profiling of developing tissue and cellular stiffness by combining AFM measurements and immunostaining, which enables the assessment of the spatiotemporal shift in stiffness in correlation with the differentiation states. Compared with the identification of tissue using traditional bright-field images (Elkin et al., 2007; Christ et al., 2010) or recent vital fluorescent dyes (Franze et al., 2011), our method is superior for the fine and consistent characterization of measuring tissues and cells. Notably, the approach described here can be applied to essentially all tissues and cell types that can be labeled by antibodies. Thus, our experimental strategy has the potential to contribute to the further understanding of the role of stiffness as an inducer of mechanical signaling in cell fate determination, not only in the developing brain but also in other tissues at both embryonic and postnatal stages.

Our systematic profiling of tissue and cellular stiffness in the developing cortex documents several fundamental findings. First, the VZ and the SVZ showed gradual increases in stiffness, although apical and intermediate progenitors did not show significant

Development (2014) 141, 3793-3798 doi:10.1242/dev.109637

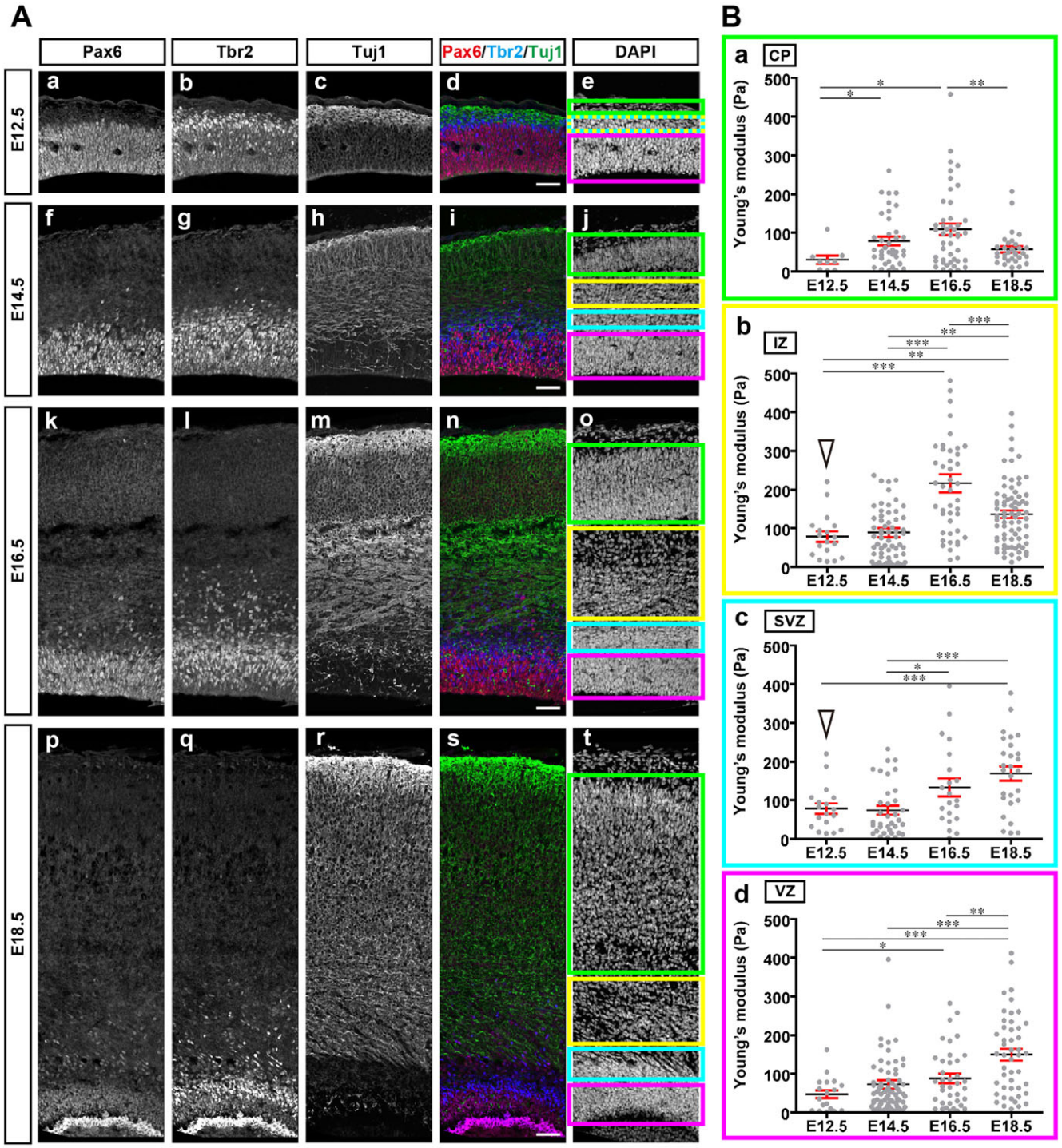

Fig. 2. Spatiotemporal measurement of tissue stiffness in the developing cortex. (A) Layers in the dorsal cortex at each embryonic stage were defined by the immunostaining of markers of neural differentiation. (d,i,n,s) Red, Pax6; blue, Tbr2; green, Tuj1. (e,j,o,t) Cortical layers were categorized as follows: Pax6-positive regions, VZ (red rectangle); regions negative for Pax6 but positive for Tbr2, SVZ (blue rectangle); regions positive for both Tbr2 and Tuj1, IZ (yellow rectangle); regions positive for only Tuj1, CP (green rectangle). Scale bars: 50 µm. (B) The Young's modulus of each layer is presented throughout the developing stages. (a) CP, (b) IZ, (c) SVZ and (d) VZ. Error bars (in red) represent the s.e.m. **P*<0.05, ***P*<0.01 and ****P*<0.001, no mark indicates a not significant result; Student's *t*-test. For E12.5, the same data are indicated for the SVZ and the IZ (arrowhead) because these layers are indistinguishable at this stage (yellow and blue dotted rectangle in Fig. 2Ae).

changes in stiffness throughout developing stages. The shift in the stiffness of those layers might correlate with the switch from neurogenesis to gliogenesis in the later stages of the development of the embryonic brain (Franze, 2013). Second, we found a peak in tissue stiffness in the IZ at E16.5 in all layers in the developing brain. Third, the stiffness of neurons increased throughout the stages of development, although the tissue stiffness of the CP decreased at E18.5. These results indicate that the shift of tissue stiffness is not always explained by the stiffness of the cells that comprise the tissue. Instead, non-cell components, such as the ECM, might affect

Development (2014) 141, 3793-3798 doi:10.1242/dev.109637

Table 1. Young's moduli of tissues and singular cells in the developing cortex

		E12.5	E14.5	E16.5	E18.5
Tissue	CP	30.1±11.0 Pa (9 points)	78.6±11.0 Pa (38 points)	108.4±14.9 Pa (45 points)	57.4±7.7 Pa (31 points)
	IZ	78.5±13.5 Pa (#) (18 points)	88.7±12.3 Pa (64 points)	216.7±23.4 Pa (44 points)	136.3±9.7 Pa (75 points)
	SVZ		74.0±11.5 Pa (35 points)	133.3±23.3 Pa (21 points)	169.3±18.7 Pa (27 points)
	VZ	46.8±10.4 Pa (18 points)	72.3±10.7 Pa (75 points)	87.8±12.3 Pa (38 points)	149.3±15.0 Pa (47 points)
Cell	Neuron	154.7±11.8 Pa (34 cells)	164.0±18.1 Pa (93 cells)	186.7±9.7 Pa (132 cells)	230.5±20.0 Pa (78 cells)
	Intermediate progenitor	146.8±29.0 Pa (9 cells)	135.7±16.9 Pa (16 cells)	127.6±34.9 Pa (6 cells)	144.6±49.1 Pa (9 cells)
	Apical progenitor	115.9±10.0 Pa (44 cells)	149.2±27.3 Pa (17 cells)	124.6±49.0 Pa (4 cells)	68.15±20.6 Pa (3 cells)

#: For time point E12.5 in tissue, the same data are indicated for the SVZ and the IZ because these layers are indistinguishable at this stage. Tissue: E12.5, two slices; E14.5, five slices; E16.5, four slices; E18.5, six slices. Cell: E12.5, 13 brains; E14.5, 16 brains, E16.5, 11 brains; E18.5, six brains. The information in brackets gives the total number of measurements made. Means±s.e.m. are shown.

the tissue stiffness. Indeed, components of the ECM are different between the layers of the dorsal cortex (Sheppard et al., 1991; Fietz et al., 2012). In addition, tissue structure, such as cellular density, and the dynamic cellular movements [i.e. neural migration in the CP (Marin et al., 2010) and interkinetic nuclear migration (Kosodo, 2012) in the VZ], might affect the tissue stiffness. Further comprehensive studies of the tissue structure and cellular and non-cellular components are needed to understand how the stiffness of tissue is determined.

MATERIALS AND METHODS

Animals

Pregnant ICR mice were purchased from Japan SLC. The mid point of the day on which the vaginal plug was detected was referred to as E0.5. All animal experiments were performed according to the Kawasaki Medical School Animal Experiment Protocol.

Preparation of cortical slices

All procedures were performed in ice-cold DMEM/F12 medium (Invitrogen) without Phenol Red (Sigma-Aldrich) and were supplemented with 2.9 mg/ml D-(+) glucose (Sigma-Aldrich). Dissected embryonic forebrains were embedded in 2% agar (Nacalai) in PBS. Brains were cut into 250-µm slices using a linear slicer (DSK, Japan). Cortical slices were selected from the middle part of the brain, including the dorsal cortex and the ganglionic eminences. One or two agar-framed slices were placed on a plastic dish that had been coated with BD Cell Tak (BD Biosciences); slices were incubated in HEPES-buffered DMEM/F12 containing N-2 supplement (Invitrogen) for 2 h in a CO_2 incubator at 37°C to adhere the slices to the dish surface.

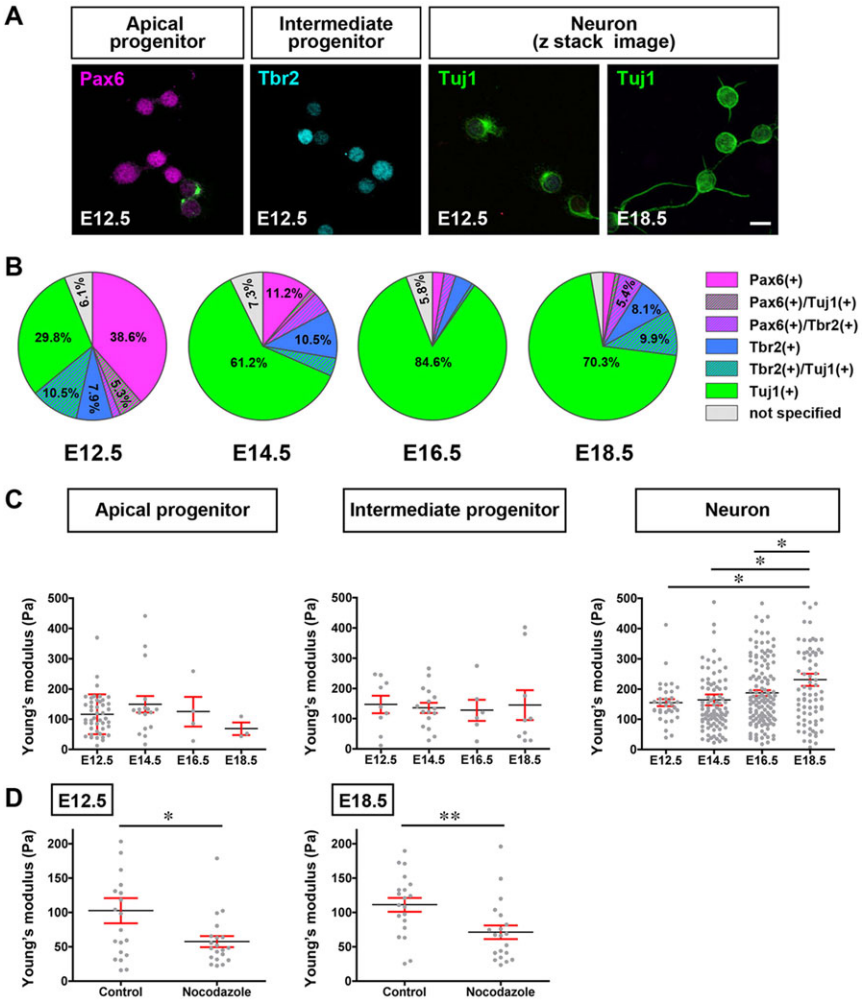

Fig. 3. Stiffness profiling of differentiating neural cells. (A) Dissociated cortical cells were immunostained after the AFM measurement and classified by markers of neural differentiation (red, Pax6, apical progenitor; blue, Tbr2, intermediate progenitor; green, Tuj1, neuron). Scale bar: 10 µm. (B) Populations of neural cells that had been dissociated from the cortex at each stage of development (E12.5, E14.5, E16.5 and E18.5). The numbers of counted cells were 114 (E12.5), 152 (E14.5), 156 (E16.5) and 111 (E18.5). Populations that comprised less than 5% of the total population are as follows. Pax6(+)/Tbr2(+), 1.8% at E12.5; Pax6(+)/Tuj1(+), 1.3%; Pax6(+)/Tb2(+), 4.6%; Tbr2(+)/Tuj1(+), 3.9% at E14.5; Pax6 positive, 2.6%; Pax6(+)/Tbr2(+), 2.6%; Tbr2 positive, 3.8%; Tbr2(+)/Tuj1(+), 0.6% at E16.5; Pax6 positive, 2.7%; Pax6(+)/Tuj1(+), 0.9%; unspecified, 2.7% at E18.5. (+)/(+) represents populations that were double positive for the indicated proteins. (C) Young's modulus values of neural cells classified by markers of the stages of development. Double positive cells were not included. (D) Interfering with microtubule polymerization reduced the stiffness of embryonic cortical cells (E12.5 and E18.5). Error bars (in red) represent s.e.m. *P<0.05, **P<0.01, no mark indicates a non-significant result; Student's t-test.

Development (2014) 141, 3793-3798 doi:10.1242/dev.109637

Preparation of living cells

Cellular dissociation from the dorsal cortex and the culture conditions are described elsewhere (Wray, 2006). Dissociated cells were plated onto a glass-bottomed dish with a grid (Matsunami) that had been coated with 15 μg/ml of poly-L-ornithine (Sigma-Aldrich) and 1 μg/ml of fibronectin (Asahi Glass). Laminin (10 μg/ml; Becton Dickinson) or type-I collagen (0.3%, Nitta Gelatin) were used instead of fibronectin for the coating test. The cell density was adjusted to 2×10^4 cells/dish. To interfere with microtubule polymerization, nocodazole (10 nM final concentration; Sigma-Aldrich) was added to the medium for 90 min before the initiation of measurements of stiffness.

AFM measurement

All measurements were performed at 37°C in the culture medium within 6 h after dissection. AFM measurement was performed using a Nanowizard II (JPK Instruments), which was mounted on an inverted microscope IX81 (Olympus). A tipless silicon cantilever with a 20 μm borosilicate bead (Novascan) was chosen for the probe because the probe type showed the best linearity depending on the indentation depth of the different probes that we tested to measure the cellular stiffness (supplementary material Fig. S1). The method used to calculate indention depths relative to cell height is given in the supplementary material methods. The spring constant of the cantilever was calibrated using the thermal noise method in air (nominal value, 0.03 N/m). The applied forces were set as 10 and 5 nN (for the slice and cell, respectively) from the calibration curve. Force-distance curves were acquired using the contact mode. The obtained force-distance curves were analyzed using the SPM image processing v.3 software (JPK instruments) (for details, see the supplementary material methods). For cortical slices, the measured points were selected in a dispersed manner in the dorsal cortex. For single-cell measurement, the bead was set on top of the soma. Prism 4 (MDF) was used for the statistical analyses.

Immunostaining

Slices and cells were immediately fixed after AFM measurement with 4% paraformaldehyde in PBS for 10 min at room temperature. The immunostaining protocol for fixed brain slices and dissociated cells is described elsewhere (Nagashima et al., 2014). The primary antibodies used were as follows: rabbit anti-Pax6 (1:500; PRB-278P, Covance), mouse anti-Tuj1 (1:500; MMS-435P, Covance), and rat anti-Eomes eFluor 660 (1:1000; 14-4875-80, eBioscience). The secondary antibodies (1:500; Molecular Probes) were Alexa 488- and Alexa 555-conjugated (A11001 and A21428, respectively). DAPI (1:500; Molecular Probes) was used for the counterstaining of nuclei. Samples were observed using a confocal laser microscope (Olympus, FV-1000).

Acknowledgements

We thank Nozomu Takata, Yoshiki Sasai, and Fumio Matsuzaki (RIKEN Center of Developmental Biology) for their support of the AFM experiments.

Competing interests

The authors declare no competing financial interests.

Author contributions

All experiments and analyses in this study were performed by M.I. M.I., N.K. and Y.K. designed and performed the AFM experiments; M.I. and K.T. performed the immunostaining; and M.I. and Y.K. designed the experiments and wrote the manuscript.

Funding

This work was funded by grants from the Japan Society for the Promotion of Science [KAKENHI 24500417]; the Uehara Memorial Foundation; the Mochida Memorial Foundation; the Takeda Science Foundation; the Kanae Foundation (to Y.K.); and Kawasaki Medical School (to M.I. and Y.K.).

Supplementary material

Supplementary material available online at
http://dev.biologists.org/lookup/suppl/doi:10.1242/dev.109637/-/DC1

References

Christ, A. F., Franze, K., Gautier, H., Moshayedi, P., Fawcett, J., Franklin, R. J. M., Karadottir, R. T. and Guck, J. (2010). Mechanical difference between white and gray matter in the rat cerebellum measured by scanning force microscopy. *J. Biomech.* **43**, 2986-2992.

DuFort, C. C., Paszek, M. J. and Weaver, V. M. (2011). Balancing forces: architectural control of mechanotransduction. *Nat. Rev. Mol. Cell Biol.* **12**, 308-319.

Elkin, B. S., Azeloglu, E. U., Costa, K. D. and Morrison, B. (2007). Mechanical heterogeneity of the rat hippocampus measured by atomic force microscope indentation. *J. Neurotraum.* **24**, 812-822.

Elkin, B. S., Ilankovan, A. and Morrison, B. (2010). Age-dependent regional mechanical properties of the rat hippocampus and cortex. *J. Biomech. Eng.* **132**, 011010.

Engler, A. J., Sen, S., Sweeney, H. L. and Discher, D. E. (2006). Matrix elasticity directs stem cell lineage specification. *Cell* **126**, 677-689.

Fietz, S. A., Lachmann, R., Brandl, H., Kircher, M., Samusik, N., Schroder, R., Lakshmanaperumal, N., Henry, I., Vogt, J., Riehn, A. et al. (2012). Transcriptomes of germinal zones of human and mouse fetal neocortex suggest a role of extracellular matrix in progenitor self-renewal. *Proc. Natl. Acad. Sci. USA* **109**, 11836-11841.

Franze, K. (2011). Atomic force microscopy and its contribution to understanding the development of the nervous system. *Curr. Opin. Genet. Dev.* **21**, 530-537.

Franze, K. (2013). The mechanical control of nervous system development. *Development* **140**, 3069-3077.

Franze, K., Francke, M., Günter, K., Christ, A. F., Körber, N., Reichenbach, A. and Guck, J. (2011). Spatial mapping of the mechanical properties of the living retina using scanning force microscopy. *Soft Matter* **7**, 3147-3154.

Fujita, S. (2003). The discovery of the matrix cell, the identification of the multipotent neural stem cell and the development of the central nervous system. *Cell Struct. Funct.* **28**, 205-228.

Gilbert, P. M., Havenstrite, K. L., Magnusson, K. E. G., Sacco, A., Leonardi, N. A., Kraft, P., Nguyen, N. K., Thrun, S., Lutolf, M. P. and Blau, H. M. (2010). Substrate elasticity regulates skeletal muscle stem cell self-renewal in culture. *Science* **329**, 1078-1081.

Götz, M. and Huttner, W. B. (2005). The cell biology of neurogenesis. *Nat. Rev. Mol. Cell Biol.* **6**, 777-788.

Götz, M., Stoykova, A. and Gruss, P. (1998). Pax6 controls radial glia differentiation in the cerebral cortex. *Neuron* **21**, 1031-1044.

Hevner, R. F., Hodge, R. D., Daza, R. A. M. and Englund, C. (2006). Transcription factors in glutamatergic neurogenesis: conserved programs in neocortex, cerebellum, and adult hippocampus. *Neurosci. Res.* **55**, 223-233.

Hoffman, B. D., Grashoff, C. and Schwartz, M. A. (2011). Dynamic molecular processes mediate cellular mechanotransduction. *Nature* **475**, 316-323.

Keung, A. J., Asuri, P., Kumar, S. and Schaffer, D. V. (2012). Soft microenvironments promote the early neurogenic differentiation but not self-renewal of human pluripotent stem cells. *Integr. Biol.* **4**, 1049-1058.

Kondra, S., Laishram, J., Ban, J., Migliorini, E., Di Foggia, V., Lazzarino, M., Torre, V. and Ruaro, M. E. (2009). Integration of confocal and atomic force microscopy images. *J. Neurosci. Methods* **177**, 94-107.

Kosodo, Y. (2012). Interkinetic nuclear migration: beyond a hallmark of neurogenesis. *Cell. Mol. Life Sci.* **69**, 2727-2738.

Leipzig, N. D. and Shoichet, M. S. (2009). The effect of substrate stiffness on adult neural stem cell behavior. *Biomaterials* **30**, 6867-6878.

Lui, J. H., Hansen, D. V. and Kriegstein, A. R. (2011). Development and evolution of the human neocortex. *Cell* **146**, 18-36.

Marin, O., Valiente, M., Ge, X. and Tsai, L.-H. (2010). Guiding neuronal cell migrations. *Cold Spring Harb. Perspect. Biol.* **2**, a001834.

Molyneaux, B. J., Arlotta, P., Menezes, J. R. L. and Macklis, J. D. (2007). Neuronal subtype specification in the cerebral cortex. *Nat. Rev. Neurosci.* **8**, 427-437.

Moore, S. W., Roca-Cusachs, P. and Sheetz, M. P. (2010). Stretchy proteins on stretchy substrates: the important elements of integrin-mediated rigidity sensing. *Dev. Cell* **19**, 194-206.

Nagashima, F., Suzuki, I. K., Shitamukai, A., Sakaguchi, H., Iwashita, M., Kobayashi, T., Tone, S., Toida, K., Vanderhaeghen, P. and Kosodo, Y. (2014). Novel and robust transplantation reveals the acquisition of polarized processes by cortical cells derived from mouse and human pluripotent stem cells. *Stem Cells Dev.* **23**, 2129-2142.

Saha, K., Keung, A. J., Irwin, E. F., Li, Y., Little, L., Schaffer, D. V. and Healy, K. E. (2008). Substrate modulus directs neural stem cell behavior. *Biophys. J.* **95**, 4426-4438.

Sheppard, A. M., Hamilton, S. K. and Pearlman, A. L. (1991). Changes in the distribution of extracellular matrix components accompany early morphogenetic events of mammalian cortical development. *J. Neurosci.* **11**, 3928-3942.

Spedden, E. and Staii, C. (2013). Neuron biomechanics probed by atomic force microscopy. *Int. J. Mol. Sci.* **14**, 16124-16140.

Spedden, E., White, J. D., Naumova, E. N., Kaplan, D. L. and Staii, C. (2012). Elasticity maps of living neurons measured by combined fluorescence and atomic force microscopy. *Biophys. J.* **103**, 868-877.

Wray, S. (2006). Culture of neuroepithelial stem cells. In *Short Protocols in Neuroscience: Cellular and Molecular Methods*, Chapter 3.1-2. New Jersey: John Wiley & Sons Inc.

Supplementary Methods

Force-distance curve analysis

Force-distance curves were acquired using contact mode. The obtained force-distance curves were analyzed using the SPM image processing v.3 software (JPK instruments). For the cantilever with a bead, the "Sphere" (1) and "Paraboloid (the original Hertz model)" (Kuznetsova et al., 2007) (2) models were applied according to the manufacturer's instruction and compared for the calculation of Young's moduli.

$$F = \frac{E}{1-\nu^2}\left[\frac{a^2+R^2}{2}\ln\frac{R+a}{R-a} - aR\right] \quad (1)$$

$$F = \frac{E}{1-\nu^2}\frac{4\sqrt{R}}{3}\delta^{3/2} \quad (2)$$

$$F = \frac{E}{1-\nu^2}\frac{2\tan\alpha}{\pi}\delta^2 \quad (3)$$

The values obtained using Equations (1) and (2) were essentially the same at the indentation depth that we examined (Figs. S3 for tissue slices and S5 for singular cells). Only the values obtained with Equation (1) are indicated, unless described in the Results and Table 1. For the sharpened pyramidal tip, Sneddon model (3) (Sneddon, 1965; Kuznetsova et al., 2007) was applied. The variables are as follows: Radius of the bead, *R*; Applied force, *F*; Young's modulus, *E*; Poisson's ratio, *v*; radius of contact

circle, a; the half-opening angle of the tip of the cantilever, α and depth of indentation, δ. The Poisson's ratio was chosen to be 0.5, as used in cellular (Kataoka et al., 2002) and tissue studies (Elkin et al., 2007).

Cell height measurement

Dissociated living cortical cells were stained with PKH26 (SIGMA) and Hoechst33258 (SIGMA) before plating according to the company's instructions. Z stack images were captured using a confocal laser microscope under incubation. The cell height was calculated from the obtained Z stack images using Volocity Visualization (Perkin-Elmer).

References

Elkin, B. S., Azeloglu, E. U., Costa, K. D. and Morrison, B., 3rd (2007) 'Mechanical heterogeneity of the rat hippocampus measured by atomic force microscope indentation', *J. Neurotraum.* 24(5): 812-22.

Kataoka, N., Iwaki, K., Hashimoto, K., Mochizuki, S., Ogasawara, Y., Sato, M., Tsujioka, K. and Kajiya, F. (2002) 'Measurements of endothelial cell-to-cell and cell-to-substrate gaps and micromechanical properties of endothelial cells during monocyte adhesion', *Proc. Nat. Acad. Sci. U. S. A.* 99(24): 15638-43.

Kuznetsova, T. G., Starodubtseva, M. N., Yegorenkov, N. I., Chizhik, S. A. and Zhdanov, R. I. (2007) 'Atomic force microscopy probing of cell elasticity', *Micron* 38(8): 824-33.

Sneddon, I. N. (1965) 'The relation between load and penetration in the axisymmetric boussinesq problem for a puncn of arbitrary profile', *Int. J. Engng. Sci.* 3: 47-57.

Supplementary figure legends

Figure S1

(**A)** Schematics of cantilevers tested in our experiments. Types of cantilevers are indicated. Grey circle, a bead attached with cantilever; grey triangle, a pyramidal shaped tip of cantilever; blue semicircle, a cortical cell on a dish.

(B) Comparison of cantilevers for measurement of the stiffness of cortical cells. The Young's modulus of the singular neural cells derived from cortices at E14.5 were measured using cantilevers with **(a)** a 20-μm (in diameter) borosilicate bead, **(b)** a 5-μm borosilicate bead, **(c)** a 4.5-μm polystyrene bead, and **(d)** a sharpened pyramidal tip (OMCL-TR400-PB, Olympus). For the fitting model for each cantilever, see the Supplemental Methods. Note that the absolute value and the linearity of the stiffness along the indentation depth differed depending on the tip shape. Among four cantilever types, (a) the 20-μm borosilicate bead exhibited the highest linearity of the stiffness along the indentation depth.

Figure S2

(A) Agar frame maintains the structure of sliced embryonic brain. A living cortical slice of E18.5 mouse brain with 2% agar frame (**b** and **d**) maintained its intact structure for 3 hours during the culture for AFM measurement. In contrast, collapsed structures were identified in the brain slice without agar frame (**a** and **c**). (c) and (d), white rectangles in (a) and (b), respectively. Arrowhead in (b), the edge of the agar frame. Arrow in (c), the collapsed structure of the cortical plate. Bar = 500 μm.

(B) Concentration of the agar does not affect to the tissue stiffness. The stiffness of E18.5 mouse brain cortical slices was measured with agar (0.5%, 2%, and 5%) or without an agar frame (20 points in each condition). Note that the brain slice without agar exhibits lower stiffness, likely reflecting the collapsed structure shown in (A). Error bars in the graphs: S.E.M. *P<0.05, **P<0.01, and ***P<0.001, no mark indicates a non-significant result, t-test.

Figure S3

Profiles between the indentation depth (0.25, 0.5, 1, 3, and 5 μm) and the obtained

Young's modulus of the cortical tissue at various developing stages (E12.5 (**a**), 14.5 (**b**), 16.5 (**c**), and 18.5 (**d**)). Upon increasing the indentation, the measured Young's modulus showed a non-linear response that decreased initially in the depth range from 0.25 to 0.5 μm and increased at depths greater than 0.5 μm. Comparison of the Young's modulus of the cortical tissue calculated by different models is displayed in each panel. The obtained force-distance curves were analyzed by the SPM image processing software using the "Sphere" and "Paraboloid" models (see the Supplemental Methods). The calculated values are almost identical (4.4% difference at maximum) at an indentation depth of 3 μm in all developing stages. The Young's moduli acquired from all layers are contained (n = 20 for each stage). Error bars in the graphs: S.E.M.

Figure S4

(A) Effect of coating conditions on the stiffness of cortical cells. Several different ECMs were used to coat plastic culture dishes to test their effect on the stiffness of E14.5 cortical cells: PLO, poly-L ornithine; FN, fibronectin; L, laminin; Col, collagen type-1. Stiffness of cortical cells on 0.3% collagen gel (1 mm in height) is indicated for

the comparison to the cellular stiffness on the plastic dish coated with poly-L ornithine + collagen. *P<0.05, **P<0.01, and ***P<0.001, no mark indicates a non-significant result, t-test.

(B) Indentation depth-dependent stiffness of the cortical cells on the fibronectin-coated dish. Stiffness of E14.5 cortical cells showed fine linearity along the indentation depth (2.5%, 5%, 10%, and 20% of cell height) on the dish coated with poly-L ornithine + fibronectin, but not with poly-L ornithine + collagen. The “Sphere” model was used for the fitting (see the Supplemental Methods). Error bars in the graphs: S.E.M.

Figure S5

Profiles between the indentation depth (2.5%, 5%, 10%, and 20% of cell height) and the obtained Young’s modulus of the single neural cells dissociated from cortices of various developing stages (E12.5 (**a**), 14.5 (**b**), 16.5 (**c**), and 18.5 (**d**). Comparison of the Young’s modulus of the single neural cells calculated by different models is displayed in each panel. The obtained force-distance curves were analyzed using the “Sphere” and “Paraboloid” models. The calculated values are almost identical (1.6% difference at

maximum) at 5% of cell height as an indentation depth in all developing stages. Note the fine linearity in the range of 2.5-10% of the cell height as an indentation depth at all developmental stages (R^2 = 0.999 (a), 0.995 (b), 0.999 (c), and 0.994 (d), the “Sphere” model). The Young’s moduli acquired from all cell types are shown (n = 30 for each stage). Error bars in the graphs: S.E.M. (b) is the same data as shown in Fig S1B (a).

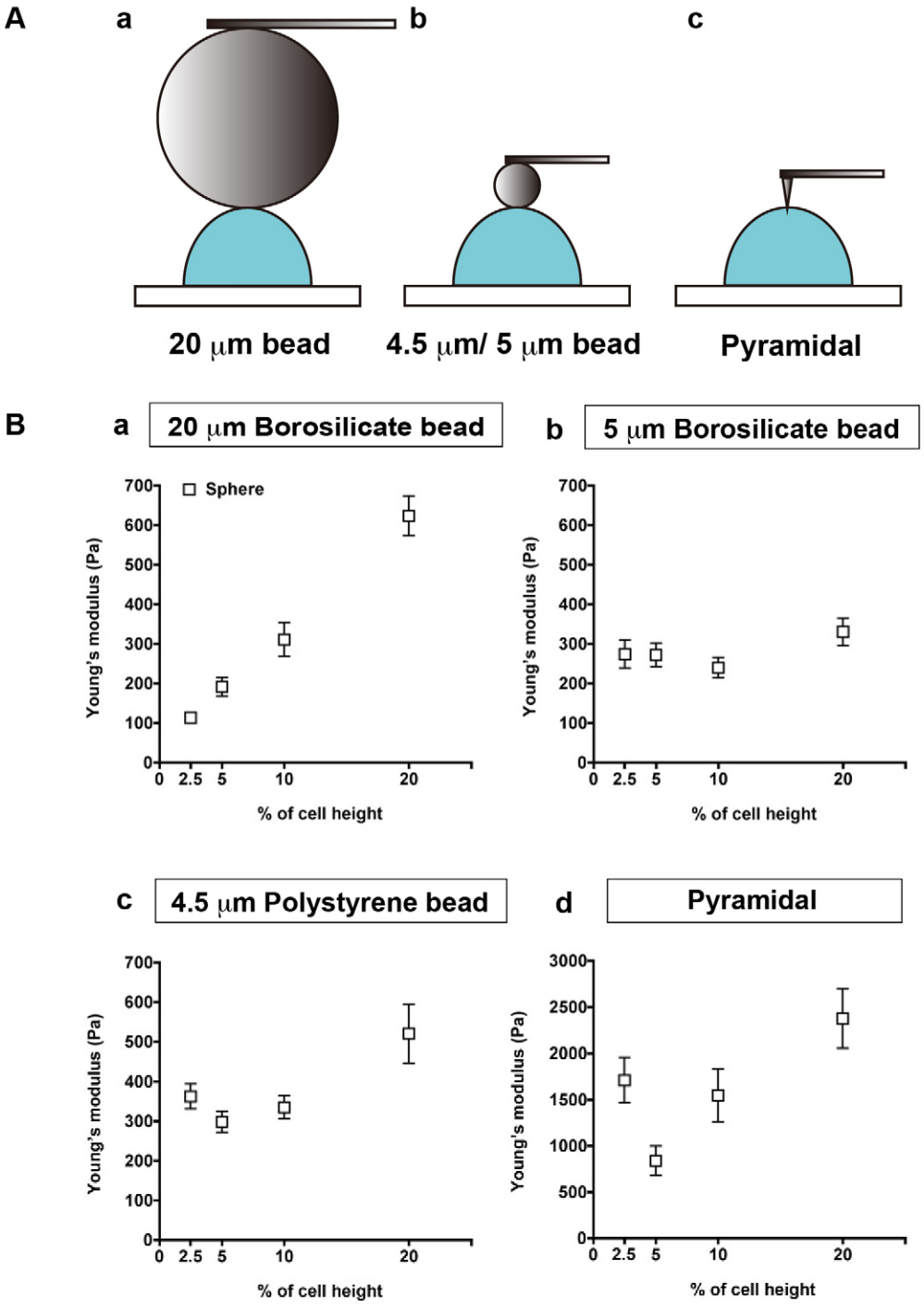

Supplemental Figure 1 Iwashita et al

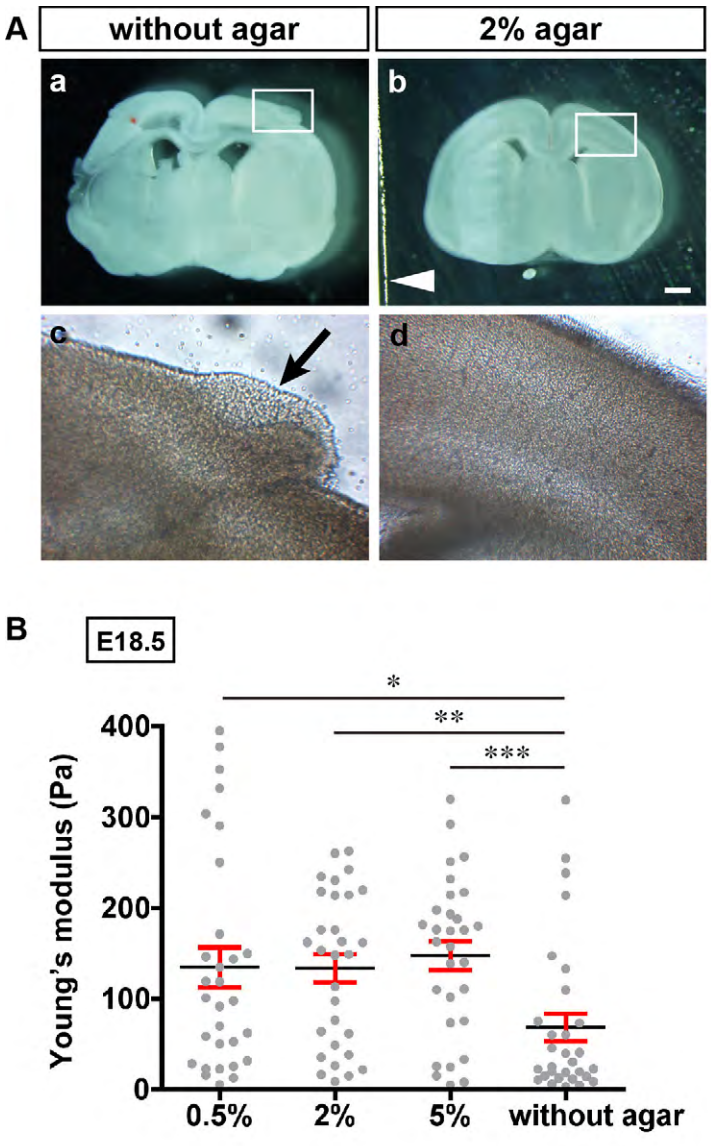

Supplemental Figure 2 Iwashita et al

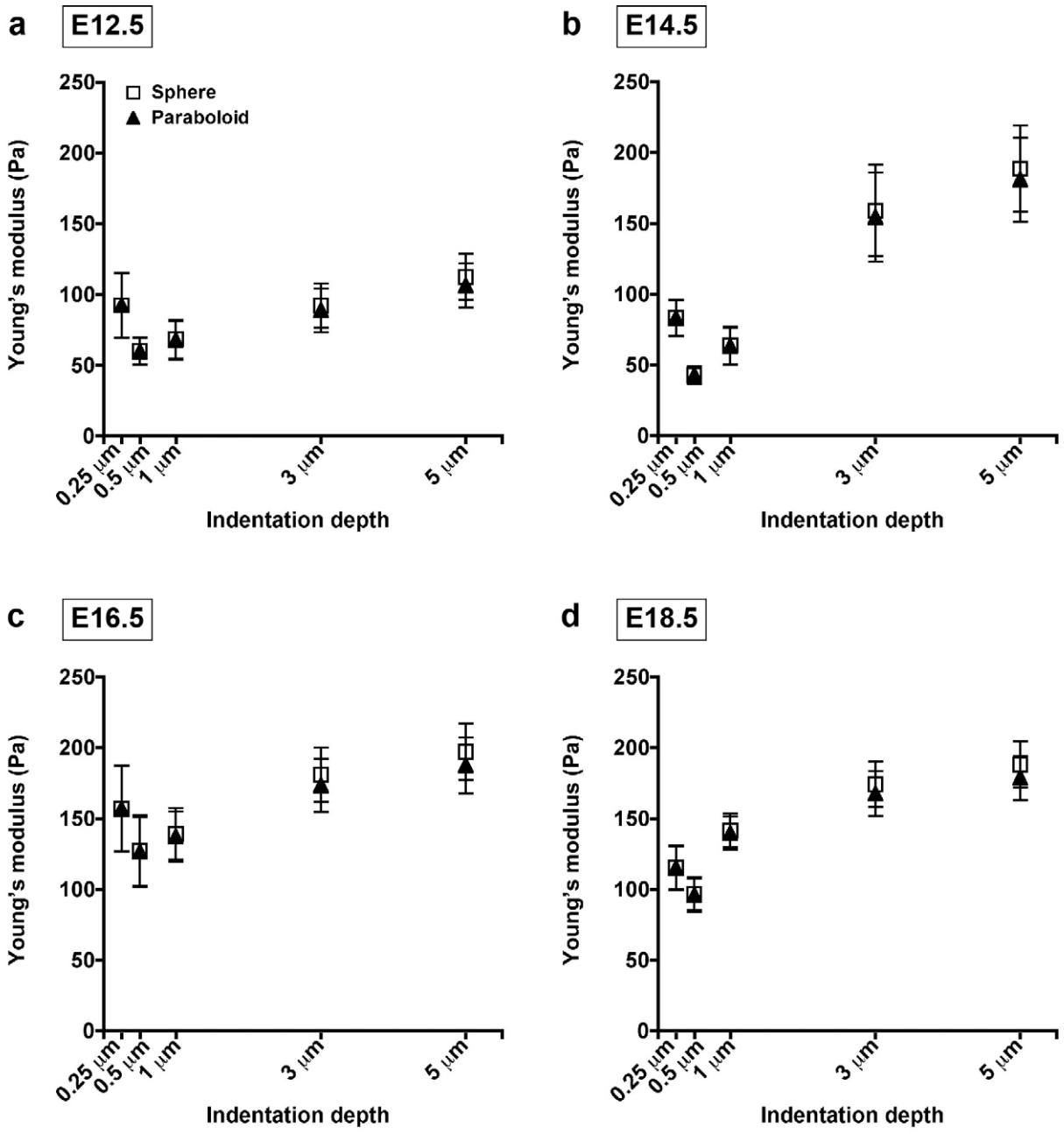

Supplemental Figure 3 Iwashita et al.

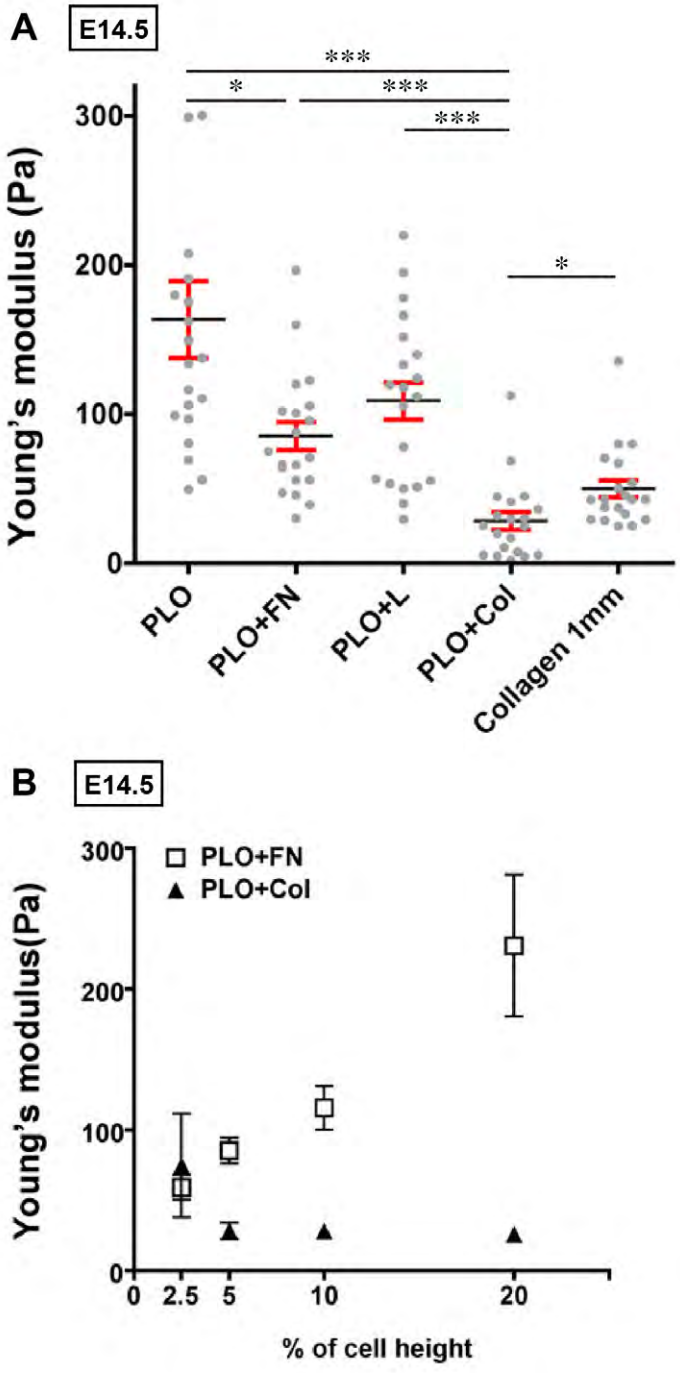

Supplemental Figure 4 Iwashita et al.

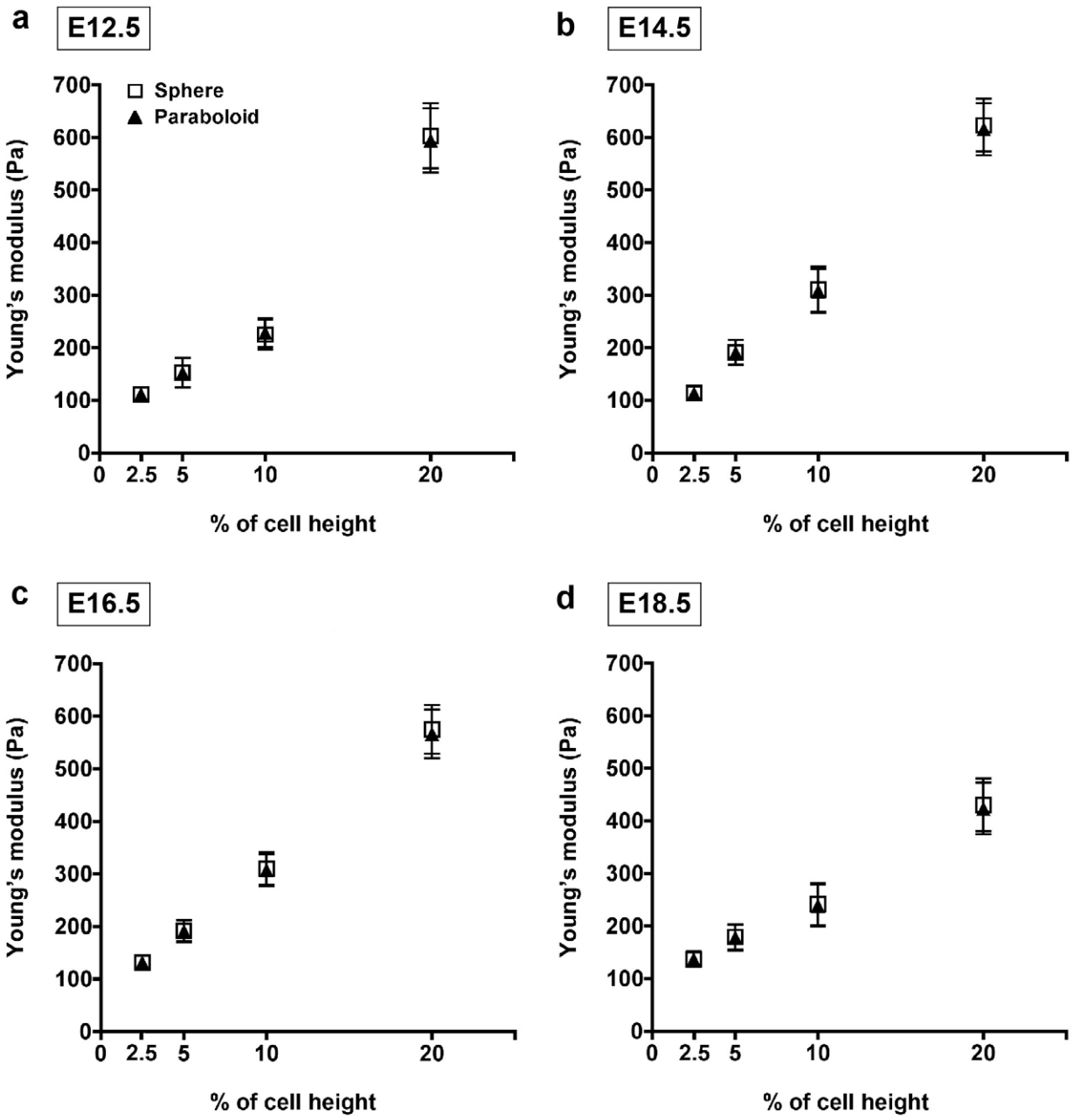

Supplemental Figure 5 Iwashita et al.